

Epithelial Ca<sup>2+</sup> channel (ECAC1) in autosomal dominant idiopathic hypercalciuria

**Müller D**, Hoenderop JGJ, Vennekens R, Eggert P, Harangi F, Mèhes K, Garcia-Nieto V, Claverie-Martin F, van Os CH, Nilius B, Bindels RJM

*Nephrol Dial Transplant* 2002; 17: 1614-1620

*Original Article*

## Epithelial Ca<sup>2+</sup> channel (ECaC1) in autosomal dominant idiopathic hypercalciuria

Dominik Müller<sup>1</sup>, Joost G. J. Hoenderop<sup>1</sup>, Rudi Vennekens<sup>2</sup>, Paul Eggert<sup>3</sup>, Ferenc Harangi<sup>4</sup>, Károly Méhes<sup>5</sup>, Victor Garcia-Nieto<sup>6</sup>, Felix Claverie-Martin<sup>6</sup>, Carel H. van Os<sup>1</sup>, Bernd Nilius<sup>2</sup> and René J. M. Bindels<sup>1</sup>

<sup>1</sup>Department of Cell Physiology, University Medical Centre Nijmegen, The Netherlands, <sup>2</sup>Department of Physiology, Katholieke Universiteit Leuven, Belgium, <sup>3</sup>Children's Hospital, University of Kiel, Germany, <sup>4</sup>Kerpel-Fronius County Children's Hospital of Pécs, Hungary, <sup>5</sup>Department of Pediatrics, MTA-PTE Research Group of Clinical Genetics, University Medical School, Pécs, Hungary and <sup>6</sup>Pediatric Nephrology and Research Units, Hospital Universitario Nuestra Señora de Candelaria, Santa Cruz de Tenerife, Spain

### Abstract

**Background.** The epithelial Ca<sup>2+</sup> channel (ECaC) exhibits the defining properties for being the gate-keeper in 1,25-dihydroxyvitamin D<sub>3</sub>-regulated Ca<sup>2+</sup> (re)absorption. Its recently cloned human orthologue (ECaC1) could, therefore, represent a crucial molecule in human disorders related to Ca<sup>2+</sup>-wasting such as idiopathic hypercalciuria (IH).

**Methods.** Fifty-seven members of nine families with IH were investigated. Phenotyping was performed by measurements of urinary Ca<sup>2+</sup> excretion, while other underlying disorders were appropriately excluded. Initially, the recently suggested locus for kidney stone-associated hypercalciuria on chromosome 1q23.3-q24 was investigated. Next, direct mutation analysis of all 15 exons of the ECaC1 gene and 2.9 kb upstream from the start codon was performed. hECaC1, heterologously expressed in human embryonic kidney 293 cells, was characterized by patch-clamp analysis.

**Results.** The mode of inheritance in the studied pedigrees is consistent with an autosomal dominant trait. Haplotype analysis did not implicate a role of the locus on chromosome 1. The coding sequence of the ECaC1 gene was not different between the affected and the non-affected family members. In the 5'-flanking region, three single nucleotide polymorphisms were encountered, but these polymorphisms were observed regardless of the affection status of the screened family members. Patch-clamp analysis of hECaC1 was performed as the putative pore region contains four non-conserved amino acid

substitutions compared with the other species. This analysis revealed the distinctive properties of ECaC, including a high Ca<sup>2+</sup> selectivity, inward rectification, and Ca<sup>2+</sup>-dependent inactivation.

**Conclusion.** These results do not support a primary role for hECaC1 in IH in nine affected families. Because of the heterogeneity of the disease, however, the involvement of ECaC1 in other subtypes of IH cannot be excluded and needs further investigation. The electrophysiological properties of hECaC1 further substantiate its prime role in Ca<sup>2+</sup> (re)absorption.

**Keywords:** calcium reabsorption; ECaC; kidney; patch-clamp; TRPV5

### Introduction

Because of the various important functions of Ca<sup>2+</sup>, disturbances of its homeostasis can result in a broad range of abnormalities. Among such disorders, idiopathic hypercalciuria (IH), defined as increased urinary excretion of Ca<sup>2+</sup> in the absence of any known underlying cause, is frequently observed. Because of the high prevalence and the close correlation to Ca<sup>2+</sup>-related stone formation, its socio-economic impact is considerable [1]. In many cases, the family history is positive and it has been suggested that in these patients, the disease is primarily inherited as an autosomal dominant trait [2]. Intensive investigations have been performed in the past to elucidate responsible mechanisms and several potential candidate genes for IH have been excluded [3–5]. In IH patients, research has centred on the uptake and excretion of Ca<sup>2+</sup>, as intestinal hyperabsorption of Ca<sup>2+</sup> could lead, via increased plasma Ca<sup>2+</sup> levels, to an increased

Correspondence and offprint requests to: René J. M. Bindels, 160 Cell Physiology, University Medical Centre Nijmegen, PO Box 9101, NL-6500 HB Nijmegen, The Netherlands. Email: r.bindels@ncmls.kun.nl

filtered load of  $\text{Ca}^{2+}$  surpassing the renal reabsorption capacity. Likewise, a primary defect of renal  $\text{Ca}^{2+}$  reabsorption could lead directly to hypercalciuria [6]. It is also noteworthy that some studies have demonstrated decreased bone density in patients with IH [7]. Additionally, a well-characterized rat model of hypercalciuria shows simultaneous alterations in  $\text{Ca}^{2+}$  handling in kidney, intestine, and bone [8]. Recently, Reed and co-workers [9,10] identified an area on chromosome 1 linked to the transmission of hypercalciuria, while another group reported suggestive evidence of a gene locus on chromosome 12 in close vicinity to the vitamin D receptor (VDR) gene. The VDR gene product itself has been extensively investigated for its involvement in  $\text{Ca}^{2+}$ -related diseases, but with inconsistent results [11]. There is considerable evidence that patients suffering from hypercalciuria might not represent a homogenous group. Moreover, theories on the pathogenesis of IH were not substantiated by identification of mutations in candidate genes expressed in kidney, intestine, bone, or other tissues.

Recently, the apical  $\text{Ca}^{2+}$  entry step facilitating transcellular  $\text{Ca}^{2+}$  transport in kidney and small intestine was identified [12]. This long-sought molecule, named epithelial calcium channel or ECAC1, is localized in the apical membrane of 1,25-dihydroxyvitamin  $\text{D}_3$  ( $1,25(\text{OH})_2\text{D}_3$ )-responsive epithelia where it functions as a high  $\text{Ca}^{2+}$  selective channel. Thus, ECAC1 possesses the defining properties of the 'guardian' of transcellular  $\text{Ca}^{2+}$  transport and might play a crucial role in  $\text{Ca}^{2+}$ -related disorders [13,14]. Subsequently, its human orthologue was cloned and its genomic localization and organization was elucidated to provide the basis for functional and mutational analyses [15,16].

In the present study, the ECAC1 coding sequence and its 5'-flanking region were screened for mutations in nine families with IH. This was followed by patch-clamp analysis, thereby providing an in-depth electrophysiological characterization of the human epithelial  $\text{Ca}^{2+}$  channel.

## Subjects and methods

### *Pedigrees and phenotyping*

Included were nine families (five spanning two generations and four spanning three generations) with a total of 57 members (29 females and 28 males). The median age of all members was 16.2 years with a range from 3.1 to 65.2 years. According to generally accepted reference values, family members with a urinary  $\text{Ca}^{2+}$  excretion of  $>0.1$  mmol/kg body weight/24 h were considered as being hypercalciuric [1]. Associated symptoms included abdominal colics, haematuria, urinary tract infections, and recurrent kidney stones, the latter revealed by history, abdominal X-ray, and/or ultrasound. Although kidney stones were age-dependent and inconsistent in their appearance, they were only encountered in hypercalciuric, but never in normocalciuric family members.

### *Biochemical analysis*

Urinary sampling was initially performed as complete 24 h collections during normal  $\text{Ca}^{2+}$ -containing diet (adults 1000 mg/day). Further control investigations were carried out either as 24 h collections or as the ratio of  $\text{Ca}^{2+}$  and creatinine of a single spot urine (normal  $<600$  mmol  $\text{Ca}^{2+}$ /mmol creatinine). Additionally, urinary  $\text{Na}^+$  (as fractional excretion, FE) and oxalate were determined. None of the patients received additional vitamin D, glucocorticoids, thiazides, furosemide, or other medications that are known to influence  $\text{Ca}^{2+}$  metabolism. Biochemical analysis for serum  $\text{Na}^+$ ,  $\text{Ca}^{2+}$ , alkaline phosphatase, creatinine and urinary  $\text{Ca}^{2+}$ ,  $\text{Na}^+$ , and creatinine were performed by means of commercial assays using an auto-analyser (Hitachi 911, Boehringer, Germany). Serum  $1,25(\text{OH})_2\text{D}_3$ , parathyroid hormone (determined as intact PTH, iPTH) were analysed by standard chromatography and RIA procedures. Urinary oxalate was determined by an enzymatic assay (Sigma Diagnostics, St Louis, MO, USA). The data were expressed as mean, median, and range. Statistical analysis was performed with the Mann-Whitney *U*-test, the level of significance was set at  $P=0.05$ .

### *Haplotype analysis*

Samples of peripheral blood were taken from all available family members and genomic DNA was isolated by means of standard procedures using a commercial DNA isolation system (Promega, Madison, WI, USA). Before investigating the ECAC1 gene, haplotype analysis was performed for two loci described in the literature (1q23.3-q24 and 12q12-14) by using the microsatellite markers D1S318 (GenBank<sup>TM</sup> Accession no. L14301), D1S196 (GenBank<sup>TM</sup> Accession no. Z16503), and D12S339 (GenBank<sup>TM</sup> Accession no. Z24131) [9,10]. Semi-automated genotyping was performed on an ABI 377 DNA Sequencer and data were analysed by Genescan 2.1 and Genotyper 2.0 software (Perkin-Elmer Applied Biosystems, Foster City, CA, USA).

### *Screening the hECAC1 gene*

DNA of 18 members of nine families (one affected and one non-affected per family) was subjected to direct mutation analysis. Oligonucleotides were selected based on the genomic sequence of hECAC1 as elucidated recently [15,16]. Because of the short intron sequence between the exons 2 and 3, 5 and 6, 9 and 10 as well as 11 and 12, they were amplified by polymerase chain reaction (PCR) and sequenced as a single fragment. For the analysis of the coding sequence, all primers were located in non-coding (intronic) regions so that the intron-exon boundaries were amplified as well. PCR purification of the products and semi-automated sequencing was performed by standard procedures. The 5' flanking region of ECAC1 was amplified by the forward primer 5'-GAGGACGAGGTAGGCAGAGAAGGGCAAGTG-3' and reverse primer 5'-AAGTTTCTGGAGTTGGCTCCCCGGCCCT-3' using a long range PCR (TAKARA, Shiga, Japan). The obtained 3 kb fragment was purified and subjected to direct sequencing using primers covering this fragment at position -2927, -2320, -1827, -1325, -817, and -447.

### Construction of the hECaCl transfection vector

The open reading frame of ECaCl was amplified by reverse transcription (RT)-PCR using human kidney cortex RNA as described previously [15]. The forward and reverse primers were located at both ends of the open reading frame (forward 5'-ATGGGGGGTTTCTACCTAAG-3' and reverse 5'-TCAAAAATGGTAGACCTCCTCTCC-3', GenBank™ Accession no. AJ271207.2). The obtained 2.3 kb product was subcloned into the pGEM T-Easy vector (Promega, Madison, WI, USA) and then cloned into the pCINeo/IRES/GFP vector [17]. The sequence identity of the hECaCl open reading frame was confirmed by sequence analysis.

### Cell culture, transfection, and electrophysiology

Human embryonic kidney cells (HEK293) were grown in DMEM containing 10% (v/v) human serum, 2 mM L-glutamine, 2 U/ml penicillin, and 2 mg/ml streptomycin at 37°C in a humidity controlled incubator with 10% CO<sub>2</sub>. HEK293 cells were transiently transfected with the pCINeo/IRES/ECaCl/GFP vector as described [17]. Cells were visually identified by their green appearance in the patch-clamp set-up. Electrophysiological methods and Ca<sup>2+</sup> measurements have been described in detail previously [17]. The standard extracellular solution ('Krebs') contained (in mM) 150 NaCl, 1 MgCl<sub>2</sub>, 10 HEPES, and 10 glucose, pH 7.4, adjusted with CsOH. To test the permeability of several monovalent cations, NaCl was replaced by an equimolar amount of KCl, LiCl, CsCl or *N*-methyl-D-glucosamine chloride (NMDG-Cl). The concentration of Ca<sup>2+</sup>, Ba<sup>2+</sup>, Sr<sup>2+</sup>, or Mn<sup>2+</sup> was varied between 1 and 30 mM as indicated in the text. The standard internal (pipette) solution contained (in mM) 20 CsCl, 100 Cs-aspartate, 1 MgCl<sub>2</sub>, 10 BAPTA, 4 Na<sub>2</sub>ATP, 10 HEPES, pH 7.2, with CsOH. In the presence of 10 mM BAPTA, 7.8 mM Ca<sup>2+</sup> was added to obtain 250 nM free Ca<sup>2+</sup> as calculated with the CaBuf program (G. Droogmans, KULeuven).

## Results

### Phenotyping and biochemical analysis

Out of the nine families, one was of Spanish, two of Hungarian, one of Danish, and five of German origin. Fourteen out of the 28 male persons and 19 out of the 29 female persons were affected by hypercalciuria (Figure 1). The difference in urinary Ca<sup>2+</sup> excretion between the affected and non-affected family members was significant ( $P < 0.001$ ). All other parameters measured in serum and urine were not significantly different between the affected and the non-affected members (Table 1). In all families, the pattern of transmission was consistent with a high-penetrance autosomal dominant mode of inheritance. Of note, it cannot be excluded that IH is a polygenic disease.

### Exclusion of chromosomes 1 and 12

Analysis for the markers on chromosome 1 (D1S318 and D1S196) was performed by haplotype analysis, which did not identify a common haplotype

segregating the affected families. This result is consistent with the formal exclusion of the above mentioned locus on chromosome 1 (Figure 1). For the region on chromosome 12, a major chromosomal discrepancy was encountered when a GenBank™ search for the marker D12S339 was performed. A full match was only obtained to a Human Genome Project working draft sequence on chromosome 3 (GenBank™ Accession no. NT\_022490.2). However, the same marker was assigned to chromosome 12 according to the Marshfield map, the GB4™ map, and the Génethon map. These findings suggest that this particular marker is not representative for the VDR locus, which has been unequivocally assigned to chromosome 12.

### Mutation analysis of hECaCl

The coding sequences of hECaCl obtained from the affected and non-affected family members did not differ from each other and were identical to the sequence deposited in the corresponding GenBank™ entry revealed by the Human Genome Project (NT\_023640.5). Furthermore, intron-exon boundaries were also without differences between individuals. The presence of heterozygous variations in the coding sequence of ECaCl were also excluded which was of special interest, as the disease is transmitted as an autosomal dominant trait. Thus, a mutation in the open reading frame of ECaCl was excluded as being the underlying cause of the disease in these patients.

Subsequently, the 5'-flanking region (3' kb) of the hECaCl gene was investigated in all family members. Three single heterozygous nucleotide changes were found at position -2806 (G/C), -1600 (G/C), and -614 (G/A). This variation in the 5'-flanking region did not correlate with the affection status. At positions -1674 to -1617, a TACA repeat was identified. The length of the repeat varied from (TACA)<sub>11</sub> to (TACA)<sub>13</sub> in the studied individuals, but was independent of the affection states. This TACA repeat, as well as the G/C polymorphism at position -1600, were located in close vicinity to an identified transcription activation consensus site, named activating protein-1 or AP-1. The G/A polymorphism at position -614 was located upstream of a putative vitamin D response element (VDRE) site as reported earlier (Figure 2) [13].

### Electrophysiological characteristics of hECaCl

Sequencing revealed that the pore region of hECaCl contains four unique amino acids that are different in all other studied species [12,15]. Therefore, the electrophysiological properties of hECaCl heterologously expressed in HEK293 cells were measured. As shown in Figure 3A and B, large currents could be measured with high intracellular Ca<sup>2+</sup> buffering in extracellular divalent free conditions, which were largely blocked by 1 mM Mg<sup>2+</sup>. In the presence of extracellular Ca<sup>2+</sup>, currents showed a highly positive reversal potential and currents in response to a negative

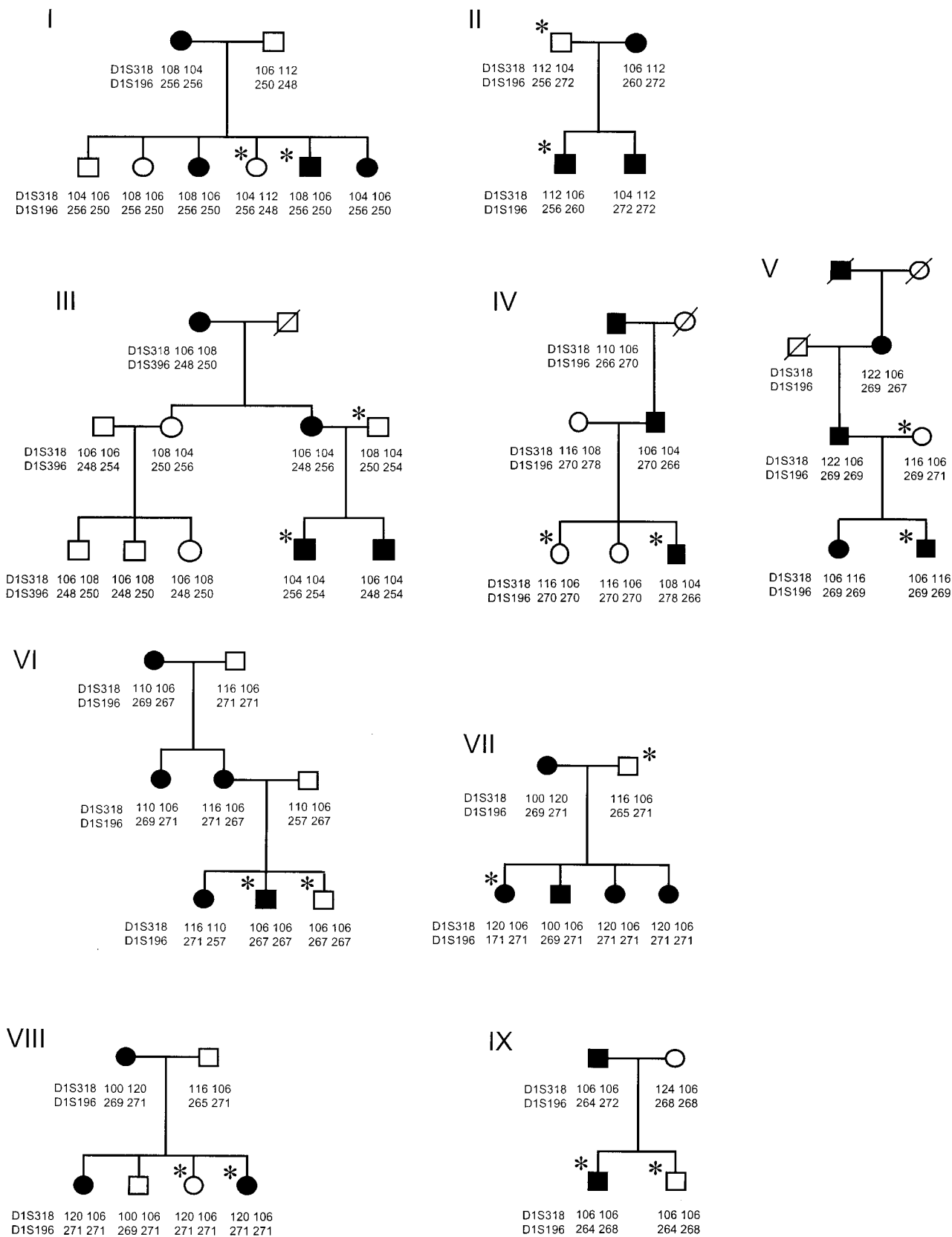


**Fig. 1.** Pedigrees of nine families. Affected individuals are marked in black, unaffected persons are indicated by unfilled symbols. Asterisks indicate individuals that were subjected to direct mutation analysis. Rectangular symbols, males; circular symbols, females. Slashed symbols represent deceased individuals. The size of the PCR fragments obtained (in base pairs) is depicted for each allele. The name of the corresponding microsatellite marker is indicated.

**Table 1.** Biochemical characteristics of the affected and non-affected family members in IH

	Affected	Non-affected	P
<i>Blood</i>			
iPTH (ng/l)	26.7 (26.9: 22.3–30.0) ( <i>n</i> = 21)	24.9 (24.8: 22.8–26.0) ( <i>n</i> = 19)	n.s.
1,25(OH) <sub>2</sub> D <sub>3</sub> (ng/l)	34.5 (36: 12–77) ( <i>n</i> = 21)	39.2 (35: 22–80) ( <i>n</i> = 17)	n.s.
Alkaline phosphatase (U/l)	231 (240: 121–326) ( <i>n</i> = 21)	219 (235: 110–271) ( <i>n</i> = 17)	n.s.
Total Ca <sup>2+</sup> (mM)	2.42 (2.41: 2.23–2.60) ( <i>n</i> = 31)	2.40 (2.41: 2.28–2.60) ( <i>n</i> = 27)	n.s.
Creatinine clearance (ml/min/1.73 qm)	113 (115: 97–123) ( <i>n</i> = 15)	115 (116: 88–122) ( <i>n</i> = 15)	n.s.
<i>Urine</i>			
Ca <sup>2+</sup> (mmol/kg/24 h)	0.22 (0.21: 0.19–0.12) ( <i>n</i> = 31)	0.06 (0.05: 0.04–0.09) ( <i>n</i> = 27)	<0.001
Oxalate (mg/1.73 qm/24 h)	53.3 (54.2: 38.3–68.7) ( <i>n</i> = 21)	57.8 (55.3: 35.6–67.8) ( <i>n</i> = 17)	n.s.
Na <sup>+</sup> (FE, %)	0.65 (0.62: 0.53–0.71) ( <i>n</i> = 21)	0.63 (0.64: 0.55–0.73) ( <i>n</i> = 17)	n.s.

Data are given as mean, median, and range. Number of individuals (*n*) included in the analysis of the different parameters is indicated between parentheses. Statistical analysis was performed using the Mann–Whitney *U*-test (n.s., not significant).

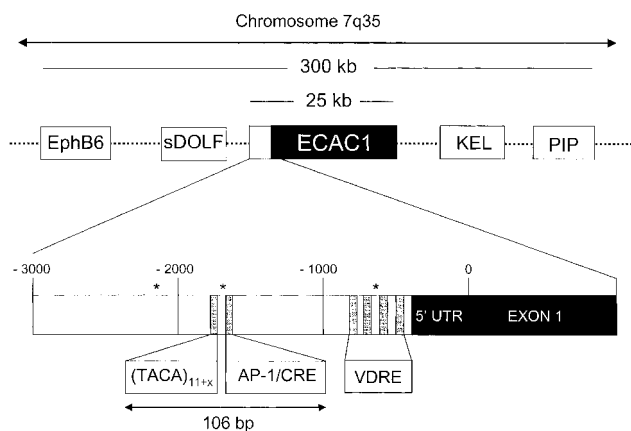


**Fig. 2.** Organization of the hECAC1 gene. The ECAC1 gene is displayed with its neighbouring genes. (sDOLF, olfactory receptor; PRSS2, protease, serine 2; PIP, prolactin-inducible protein; KEL, Kell blood group antigen.) The size of the genes as displayed does not correspond to the actual size. The 5'-flanking area with different putative regulatory sites is displayed in the inset. The sites of genetic variations are marked by an asterisk (\*), for exact locations see text. (AP-1: activating protein 1, CRE: cAMP response element.)

voltage step showed inactivation (Figure 3C–E). Monovalent currents through ECAC1 showed a conductance sequence of  $\text{Na}^+ > \text{Li}^+ \sim \text{K}^+ > \text{Cs}^+ \gg \text{NMDG}^+$  as measured from voltage ramps at  $-80$  mV. This sequence defines the Eisenman XI permeation type indicating a high ionic strength-binding site (Figure 4A and B). As  $\text{Ca}^{2+}$ -dependent inactivation was most pronounced at negative potentials, current densities were measured at 0 mV as shown in Figure 4. In this way, a sequence of channel conductance for bivalent cations of  $\text{Ca}^{2+} > \text{Ba}^{2+} \sim \text{Sr}^{2+} > \text{Mn}^{2+}$  was obtained.

## Discussion

In the present study, mutations in the hECAC1 gene, consisting of 15 exons and 3 kb of the 5'-flanking region, were not identified in nine families with IH. This finding does, therefore, not support a primary role for hECAC1 in the pathogenesis of IH in the studied

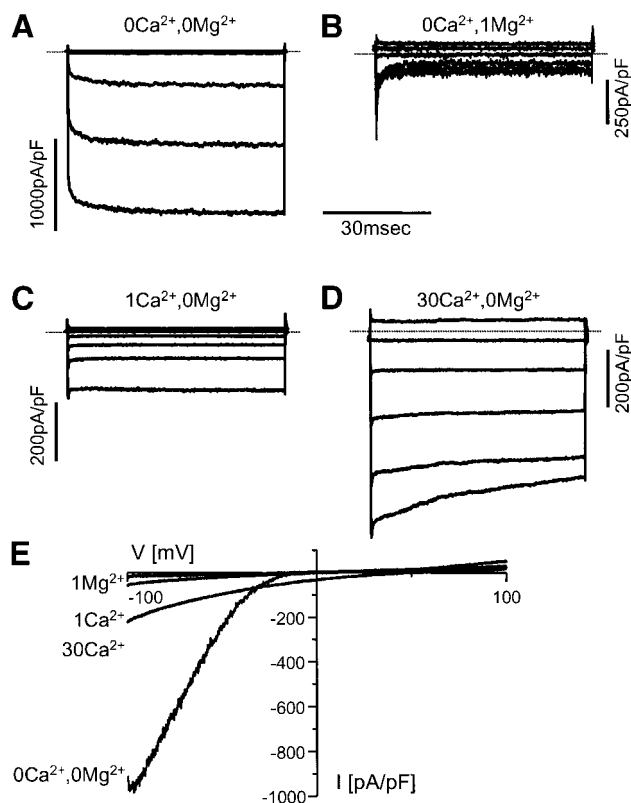


**Fig. 3.** Currents through hECAC1 heterologously expressed in HEK293 cells. (A–D) Representative examples of currents in response to a series of voltage step from +40 to  $-140$  mV with 40 mV decrement (duration is 60 ms,  $V_H = +20$  mV). Traces were recorded in various extracellular solutions as indicated in millimolar. Notice the different scaling between the panels. Cells were loaded with 10 mM BAPTA through the pipette solution. (E) Current traces in response to a ramp protocol from  $-100$  to  $+100$  mV (duration is 400 ms,  $V_H = +20$  mV) in the presence of various concentrations of  $\text{Ca}^{2+}$  and  $\text{Mg}^{2+}$ , as indicated.

families, but ECAC1 cannot be excluded as a candidate gene in other families with IH as the pathogenesis of the disease is heterogenous.

Before the ECAC1 gene was investigated in our families, two loci recently suggested to play a role in  $\text{Ca}^{2+}$  stone-associated hypercalciuria were evaluated [9,10]. A trait associated with intestinal  $\text{Ca}^{2+}$

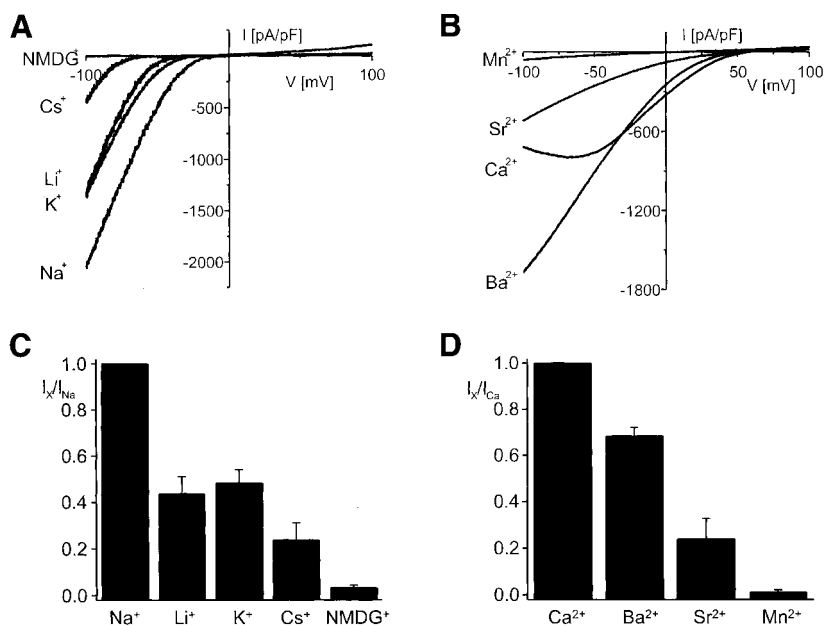


**Fig. 4.** Mono and divalent selectivity of hECaCl heterologously expressed in HEK293 cells. (A) Representative current traces in response to a voltage-ramp protocol as in Figure 3. Currents were recorded in the absence of extracellular divalents with Na<sup>+</sup>, Li<sup>+</sup>, K<sup>+</sup>, Cs<sup>+</sup>, or NMDG<sup>+</sup> as the charge carrier, as indicated. (B) Pooled data from six cells comparing mean current densities recorded at -80 mV from voltage ramps as above with different monovalent ions as the charge carrier. (C) Representative current traces in response to a reverse voltage-ramp protocol from +100 to -100 mV (duration 400 ms, V<sub>H</sub> = +20 mV). Currents were recorded in the absence of extracellular Mg<sup>2+</sup> and in the presence of 150 mM Na<sup>+</sup> and 10 mM of Ca<sup>2+</sup>, Ba<sup>2+</sup>, Sr<sup>2+</sup>, and Mn<sup>2+</sup>. (D) Pooled data comparing mean current densities recorded at 0 mV (for details see results section; n = 2–8).

hyperabsorption in a severe form of absorptive hypercalciuria has been mapped to chromosome 1q23.3-q24 [9]. The markers used were sufficient to reveal a two-point LOD score of 3.3 and analysis of the family members mapped the affected gene to a 4.3 Mb region between markers D1S2681 and D1S2815. In the present study, however, this locus on chromosome 1 could not be associated with IH by haplotype analysis using markers located within the designated region. In addition, the VDR locus on chromosome 12q12-q14 was implicated in a cohort of large French Canadian pedigrees with IH using four markers spanning a region of 11.2 cM [10]. However, the discriminating marker D12S339 has been assigned simultaneously to chromosomes 3 and 12. The VDR locus has, therefore, not been included as candidate gene in the present study.

It is generally known that IH, even the autosomal dominant form, is genetically heterogeneous. This is further substantiated by the present impossibility to confirm the assignment of a previously identified locus on chromosome 1. Because of the existing heterogeneity within subgroups of IH patients, direct mutation analysis was performed on the ECAC1 gene. The coding region of the ECAC1 gene did not contain mutations in the affected family members. Screening was then extended by analysing the nucleotide sequence 3 kb upstream of exon 1. This was of interest as there is increasing evidence that diseases are not only caused by mutations in the open reading frame of a gene, but also by variations of the respective

promoter area. For instance, variations in the promoter influence the function of ion channels in *Drosophila* [18]. In addition, it was shown that a mutation in the coding sequence of human cystic fibrosis transmembrane regulator (CFTR) resulted in a different phenotype if associated with a naturally occurring allelic variation in the promoter [19]. Interestingly, the 5'-flanking area of human ECAC1 contains several consensus sites for the binding of transcription factors including four VDREs. Accordingly, it was demonstrated that 1,25(OH)<sub>2</sub>D<sub>3</sub> regulates the expression of ECAC1 in the kidney on the transcriptional level [13]. There were, however, no mutations observed in this promoter region. We encountered a TACA repeat, which showed variation in length among the family members. This repeat is located 55 bp upstream of an AP-1 and cAMP response element consensus site (TGACGTCA) and might interfere with binding of the corresponding transcription factor. As functional data on the 5'-flanking region of ECAC1 are lacking so far, it might be possible that other, yet unknown, sequences upstream or downstream of the ECAC1 gene influence transcriptional activity and might represent a putative target for future mutational analysis.

The otherwise conserved pore-forming region of hECaCl contains four unique amino acids (T532, V540, A543, D548) which are not present in the sequence of other species [12,15]. The critical role of the single pore residue, D542, for proper Ca<sup>2+</sup> gating in rabbit ECaCl was recently demonstrated [20]. It

was, therefore, of importance to address the functional characteristics of the non-conserved pore region of hECaC1. Patch-clamp analysis demonstrated that hECaC1 exhibits the distinctive properties for being the prime molecule in transcellular  $\text{Ca}^{2+}$  (re)absorption. ECaC1 is constitutively activated, displays inward rectifying currents at negative membrane potentials, and exhibits a high  $\text{Ca}^{2+}$  selective permeability. The channel has also  $\text{Ca}^{2+}$ -dependent autoregulatory mechanisms, including fast inactivation and inhibition by elevated intracellular  $\text{Ca}^{2+}$  concentrations. With special regard to the unique amino acids in the pore-forming region of hECaC1, the electrophysiological characteristics appeared to be similar to those of rabbit ECaC1 [20]. This suggests that the four variant amino acids are not critical for  $\text{Ca}^{2+}$  gating, at least not in the experimental set-up used in this study. The question why this variation only occurs in human ECaC1 whereas the other transcripts of the ECAC family are fully conserved in this area, even across the borders of species, remains unexplained.

In summary, we could not implicate the ECaC1 gene in IH in nine affected families. Because of the heterogeneity of the disease, however, the involvement of ECaC1 in other subtypes of IH cannot be excluded and needs further investigation.

**Acknowledgements.** The authors thank Drs B. van den Heuvel and N. Knoers for their help with the haplotype analysis. D.M. was supported by a grant of the Deutsche Forschungsgemeinschaft (MU 1497 2-1). This work was supported by a grant from the Dutch Organisation of Scientific Research (NWO-ALW 810.38.004, Zon-Mw 016.006.001), the Belgian Federal Government, the Flemish Government and the Onderzoeksraad KU Leuven (GOA 99/07, F.W.O. G.0237.95, F.W.O. G.0214.99, F.W.O. G. 0136.00), the Interuniversity Poles of Attraction Program IUAP Nr.3P4/23 and a grant from the 'Alphonse and Jean Forton—Koning Boudewijn Stichting' R7115 B0.

## References

- Asplin JR, Favus MJ, Coe FL. Nephrolithiasis. In: Brenner BM, ed. *The Kidney*. 5th edn. WB Saunders, Philadelphia, 1984; 1893–1935
- Coe FL, Parks J, Moore ES. Familial idiopathic hypercalciuria. *N Engl J Med* 1979; 300: 337–400
- Scott P, Ouimet D, Proulx Y *et al.* The  $1\alpha$ -hydroxylase locus is not linked to  $\text{Ca}^{2+}$  stone formation or calciuric phenotypes in French-Canadian families. *J Am Soc Nephrol* 1998; 9: 425–432
- Petrucchi M, Scott P, Ouimet D *et al.* Evaluation of the calcium-sensing receptor gene in idiopathic hypercalciuria and calcium nephrolithiasis. *Kidney Int* 2000; 58: 38–42
- Scheinmann SJ, Cox JPD, Lloyd SE *et al.* Isolated hypercalciuria with mutation in CLCN5: relevance to idiopathic hypercalciuria. *Kidney Int* 2000; 57: 232–239
- Santos F, Súrez D, Málaga S, Crespo M. Idiopathic hypercalciuria in children: pathophysiologic considerations of renal and absorptive subtypes. *J Pediatr* 1987; 110: 238–243
- García-Nieto V, Ferrández C, Monge M, de Sequera M, Dolores Rodrigo M. Bone mineral density in paediatric patients with idiopathic hypercalciuria. *Pediatr Nephrol* 1997; 1: 578–583
- Krieger NS, Stathopoulos VM, Bushinsky DA. Increased sensitivity to  $1,25(\text{OH})_2\text{D}_3$  in bone from genetic hypercalciuric rats. *Am J Physiol* 1996; 271: C130–C135
- Reed BY, Heller HJ, Gitomer WL, Pak CYC. Mapping of a gene defect in absorptive hypercalciuria to chromosome 1q23.3-q24. *J Clin Endocrinol Metab* 1999; 84: 3907–3913
- Scott P, Ouimet D, Valiquette L *et al.* Suggestive evidence for a susceptibility gene near the vitamin D receptor locus in idiopathic calcium stone formation. *J Am Soc Nephrol* 1999; 10: 1007–1013
- Yao J, Kathpalia P, Bushinsky DA, Favus MJ. Hyperresponsiveness of vitamin D receptor gene expression to  $1,25$ -dihydroxyvitamin  $\text{D}_3$ . *J Clin Invest* 1998; 101: 2223–2332
- Hoenderop JGJ, van der Kemp AWCM, Hartog A *et al.* Molecular identification of the apical  $\text{Ca}^{2+}$  channel in  $1,25$ -dihydroxyvitamin  $\text{D}_3$ -responsive epithelia. *J Biol Chem* 1999; 274: 8375–8378
- Hoenderop JGJ, Müller D, Hartog A *et al.* Calcitriol controls the epithelial calcium channel in kidney. *J Am Soc Nephrol* 2001; 12: 1342–1349
- Vennekens R, Hoenderop JGJ, Prenen J *et al.* Permeation and gating properties of the novel Epithelial  $\text{Ca}^{2+}$  channel. *J Biol Chem* 2000; 275: 3963–3969
- Müller D, Hoenderop JGJ, Meij IC *et al.* The human epithelial calcium channel (ECaC1): cloning, tissue distribution and chromosomal mapping. *Genomics* 2000; 7: 48–53
- Müller D, Hoenderop JGJ, van Os CH, Bindels RJM. The epithelial calcium channel (ECaC1): molecular details of a novel player in renal calcium handling. *Nephrol Dial Transplant* 2001; 16: 1329–1335
- Nilius B, Oike M, Zahradnik I, Droogmans G. Activation of a  $\text{Cl}^-$  current by hypotonic volume increase in human endothelial cells. *J Gen Physiol* 1994; 103: 787–805
- Atkinson NS, Brenner R, Chang WM, Wilbur J, Larimer JL, Yu J. Molecular separation of two behavioral phenotypes by a mutation affecting the promoter of a  $\text{Ca}^{2+}$ -activated K channel. *J Neurosci* 2000; 20: 2988–2993
- Romey MC, Pallares-Ruiz N, Mange A *et al.* A naturally occurring sequence variation that creates a YY1 element is associated with increased cystic fibrosis transmembrane conductance regulator gene expression. *J Biol Chem* 2000; 275: 3561–3567
- Nilius B, Vennekens R, Prenen J, Hoenderop JGJ, Droogmans G, Bindels RJM. The single pore residue Asp542 determines  $\text{Ca}^{2+}$  permeation and  $\text{Mg}^{2+}$  block of the epithelial  $\text{Ca}^{2+}$  channel. *J Biol Chem* 2001; 276: 1020–1025

Received for publication: 19.12.01

Accepted in revised form: 26.4.02